Rab31 and APPL2 enhance FcγR-mediated phagocytosis through PI3K/Akt signaling in macrophages

Jeremy C. Yeo, Adam A. Wall, Lin Luo, and Jennifer L. Stow
Institute for Molecular Bioscience, University of Queensland, Brisbane QLD 4072, Australia

ABSTRACT **Membrane remodeling in the early stages of phagocytosis enables the engulfment of particles or pathogens and receptor signaling to activate innate immune responses. Members of the Rab GTPase family and their disparate effectors are recruited sequentially to regulate steps throughout phagocytosis. Rab31 (Rab22b) is known for regulating post-Golgi trafficking, and here we show in macrophages that Rab31-GTP is additionally and specifically recruited to early-stage phagosomes. At phagocytic cups, Rab31 is first recruited during the phosphoinositide transition from PI(4,5)P_2 to PI(3,4,5)P_3, and it persists on PI(3)P-enriched phagosomes. During early phagocytosis, we find that Rab31 recruits the signaling adaptor APPL2. siRNA depletion of either Rab31 or APPL2 reduces FcγR-mediated phagocytosis. Mechanistically, this corresponds with a delay in the transition to PI(3,4,5)P_3 and phagocytic cup closure. APPL2 depletion also reduced PI3K/Akt signaling and enhanced p38 signaling from FcγR. We thus conclude that Rab31/APPL2 is required for key roles in phagocytosis and prosurvival responses of macrophages. Of interest, in terms of localization and function, this Rab31/APPL2 complex is distinct from the Rab5/APPL1 complex, which is also involved in phagocytosis and signaling.**

Monitoring Editor
Keith E. Mostov
University of California, San Francisco

Received: Oct 20, 2014
Revised: Dec 19, 2014
Accepted: Dec 30, 2014

INTRODUCTION

Macrophages are professional phagocytes of the innate immune system, entrusted with the detection and removal of pathogens, dead cells, and debris, which are taken up into phagosomes for destruction (Flannagan *et al.*, 2012). The early stages of phagocytosis are often highly actin dependent for the extension of filopodia or membrane ruffles that are used initially to contact and envelope the "prey" (Patel and Harrison, 2008). In turn, polymerization of F-actin at initial sites of phagocytosis is dependent on enrichment of phosphatidylinositol 4,5-bisphosphate (PI(4,5)P_2) in the inner leaflet of the plasma membrane (Scott *et al.*, 2005). Conversion of PI(4,5)P_2 to phosphatidylinositol 3,4,5-triphosphate (PI(3,4,5)P_3) and phosphatidylinositol 3,4-bisphosphate (PI(3,4)P_2) accompanies the closure of phagocytic cups, the disassembly of F-actin, and signaling generated by clustered Fcγ receptors (FcγRs; Dewitt *et al.*, 2006; Haglund and Welch, 2011; Jaumouillé *et al.*, 2014).

Members of the Rab family of small GTPases are pivotal to phagocytosis, and multiple Rabs and their effectors are recruited progressively throughout the process (Stein *et al.*, 2012; Gutierrez, 2013). Rab35, for instance, is one of the early Rabs enriched at the cell surface at points of phagocytic initiation. Rab35 recruits Arf6, Rac1, and Cdc42 for early actin assembly and phagocytic cup formation (Shim *et al.*, 2010; Egami *et al.*, 2011). Rab5, Rab11, and Rab7 mediate the fusion of early, recycling, and late endosomes, respectively, during phagosome maturation (Cox *et al.*, 2000; Murray *et al.*, 2005a; Silver and Harrison, 2011). Rab5 isoforms in particular have multiple roles, most notably in phagosome maturation and signaling by recruiting a series of effectors including VPS34, Hrs, EEA1, and phosphoinositide kinases and phosphatases (Fratti *et al.*, 2001; Vieira *et al.*, 2003; Kinchen *et al.*, 2008; Bohdanowicz *et al.*, 2012).

Rab31 (also known as Rab22b) is characterized, along with Rabs 21 and 22a, as a member of the Rab5 subfamily (Diekmann *et al.*, 2011). Rab31 localizes to endocytic compartments and functions in

This article was published online ahead of print in MBoC in Press (http://www.molbiolcell.org/cgi/doi/10.1091/mbc.E14-10-1457) on January 7, 2015.
The authors declare no conflict of interest.
Address correspondence to: Jennifer L. Stow (j.stow@imb.uq.edu.au).
Abbreviations used: APPL, adaptor protein, phosphotyrosine interaction, PH domain, and leucine zipper–containing; BMM, bone marrow–derived macrophage; FcγR, Fcγ receptor; IgG, immunoglobulin G; sRBC, sheep red blood cell.

the post-Golgi, endocytic or exocytic trafficking of the GLUT4 glucose transporter in adipocytes and to the epidermal growth factor receptor (EGFR) and mannose 6-phosphate receptors in epithelial cells and neurons (Ng *et al.*, 2009; Rodriguez-Gabin *et al.*, 2010; Chua and Tang, 2014). A study on Rab–effector interactions elucidated a novel structural motif functioning in interactions between Rab31 and the adaptor protein, phosphotyrosine interaction, PH domain, and leucine zipper–containing 2 (APPL2; King *et al.*, 2012). The APPL1 and -2 isoforms are multifunctional adaptors that often bind to receptors and Rabs, notable for their ability to sway the location-dependent signaling output of ligand-activated receptors (Miaczynska *et al.*, 2004; Schenck *et al.*, 2008; Zoncu *et al.*, 2009).

Proteomic and localization screens have documented Rab31 as one of multiple Rabs found on phagosomes during the uptake of different pathogens and opsonized particles (Smith *et al.*, 2007; Jutras *et al.*, 2008; Seto *et al.*, 2011), but its function in phagocytosis is still undefined. The studies described in this article were prompted by the need to gain further insights into the functions of Rab31 and its binding partners in macrophages during FcγR-mediated phagocytosis. Here we demonstrate recruitment and functional roles for Rab31, with APPL2 as its effector, on early phagosomes in macrophages. Our findings suggest that a neat juxtaposition of Rabs and APPLs with opposing functions regulates FcγR-mediated signaling.

RESULTS

GTP-Rab31 is recruited to early phagosomes

The murine macrophage cell line RAW 264.7 and primary bone marrow–derived murine macrophages (BMMs) were presented with immunoglobulin G–opsonized latex beads (IgG beads) to examine localization of Rab31 during FcγR-mediated phagocytosis (Figure 1). By immunostaining, concentrated labeling of endogenous Rab31 can be seen around actin-rich phagosomes surrounding beads in primary BMMs (Figure 1A). Transient expression of green fluorescent protein (GFP)–Rab31 in RAW 264.7 macrophages revealed similar labeling of actin-rich phagosomes, in particular those near the cell surface (Figure 1B). When examined at early (10 min) and late (30 min) time points, we found abundant labeling of GFP-Rab31 on phagosomes in the cell periphery after the onset of bead uptake, but internalized phagosomes were generally devoid of GFP-Rab31, with fluorescence plots confirming this observation (Figure 1C). The early localization of Rab31 during phagocytosis was highlighted by its comparison to the acquisition of the late endosome/lysosome marker LAMP1—typical of mature phagolysosomes—with quantification showing GFP-Rab31 and mCherry-LAMP1 enrichment on phagosomes being largely mutually exclusive (Figure 1D). Together these results show that Rab31 is recruited to newly forming, actin-rich phagosomes at the cell surface but is lost during maturation, disappearing before the conversion into phagolysosomes.

Live-cell imaging of macrophages engulfing IgG-opsonized sheep red blood cells (IgG-sRBCs) was performed to examine the dynamics of Rab31 recruitment to phagosomes. Cells were transfected with GFP-labeled, wild-type Rab31, the constitutively active mutant of Rab31 (GFP-Rab31Q64L), or the dominant-negative mutant of Rab31 (GFP-Rab31S19N; Figure 1E). Panels from time-lapse microscopy show that wild-type GFP-Rab31 was recruited directly from the cytoplasm to the phagocytic cup membranes at the cell surface, appearing within 10 s of the onset of IgG-sRBC phagocytosis. Of note, GFP-Rab31 was only recruited to the immediate site of phagocytosis and not elsewhere on the plasma membrane. GFP-Rab31 surrounded the phagosome in a circumferential manner and dissociated directly from these membranes at ~8–10 min under this regime. The constitutively active mutant of Rab31 (GFP-Rab31Q64L) was recruited in a similar manner to early phagosomes, although it persisted for longer on the membrane than its wild-type counterpart (Figure 1E). Conversely, the dominant-negative mutant (GFP-Rab31S19N) did not bind to phagosomal membranes (Figure 1E). Fluorescence quantification confirmed that wild-type Rab31 had a transient association with phagosomes but that constitutively active Rab31 remained bound to the phagosome (Figure 1E). These results overall are consistent with the temporal recruitment of cytoplasmic Rab31 to early phagosomal membranes in a GTP-dependent manner, whereas its return to the cytoplasm required the hydrolysis of GTP during phagosome maturation.

Rab31 is recruited to early phagocytic cups during the transition from $PI(4,5)P_2$ to $PI(3,4,5)P_3$

Distinct phosphoinositide species are sequentially enriched during phagosome formation and maturation, and this can be elegantly portrayed using a variety of fluorescent phosphoinositide probes (Grinstein, 2010; Bohdanowicz and Grinstein, 2013). Using a similar approach, we examined the phospholipid context for Rab31 recruitment in cells cotransfected with mCherry-PLCδ1-PH as a marker of plasma membrane $PI(4,5)P_2$, GFP-Akt-PH as a marker for $PI(3,4,5)P_3$ and $PI(3,4)P_2$, or mCherry-2XFYVE as a marker for the endosomal species, phosphatidylinositol 3-phosphate (PI(3)P; Figure 2). During phagocytosis of IgG-sRBC, mCherry-PLCδ1-PH labeling was canonically present on the plasma membrane and surface ruffles in the vicinity of attached IgG-sRBC (Figure 2, asterisk). GFP-Rab31 was first seen on a subset of $PI(4,5)P_2$ membranes at sites of direct contact with the IgG-sRBC and not on surrounding $PI(4,5)P_2$ plasma membrane/ruffle domains (Figure 2A). mCherry-PLCδ1-PH dissociated from phagosomes as GFP-Rab31 accumulated, and their inverse relationship is evident in the fluorescence intensity plot.

Receptor engagement causes the transient elevation of the signaling phosphoinositide, $PI(3,4,5)P_3$, recognized by GFP-Akt-PH. When Rab31 was compared with GFP-Akt-PH, both were recruited to $PI(3,4,5)P_3$ phagosomal membranes, but GFP-Akt-PH peaked a full minute earlier than mCherry-Rab31, shown by sequential images and by the corresponding fluorescence plot (Figure 2B). GFP-Rab31 was recruited to the phagosomes before the appearance of mCherry-2XFYVE, which denotes the conversion of the internalizing phagosomal membrane to PI(3)P (Figure 2C). After the phagosome began to acquire PI(3)P, both GFP-Rab31 and mCherry-2×FYVE persisted together for a 3-min window, as shown by sequential images and quantification of the phagosome fluorescence intensities. A schematic representation of the fluorescence intensity plots (Figure 2D) portrays GFP-Rab31 being gradually enriched during $PI(4,5)P_2$ depletion and $PI(3,4,5)P_3$ formation on the phagosome. This preceded the acquisition of early endosomal PI(3)P, and Rab31 is thus on phagosomes coincident with $PI(3,4,5)P_3$, $PI(3,4)P_2$, and PI(3)P, which often constitute signaling and trafficking domains on endosomes and phagosomes (Burd and Emr, 1998; Lu *et al.*, 2012).

The separation of GFP-Rab31 on the phagosome membrane from the surrounding plasma membrane ruffles that are enriched in $PI(4,5)P_2$ suggests that Rab31 was exclusively recruited to phagosomal membranes after particle attachment and during closure. To confirm this, we performed immunogold labeling and cryo–electron microscopy to localize GFP-Rab31. Gold labeling of GFP-Rab31 heavily decorated phagosomes around beads near the cell surface during the early stages of internalization (Figure 3). Linear GFP labeling appeared on the phagosome and on internal membrane invaginations, associated with initial phagosome remodeling

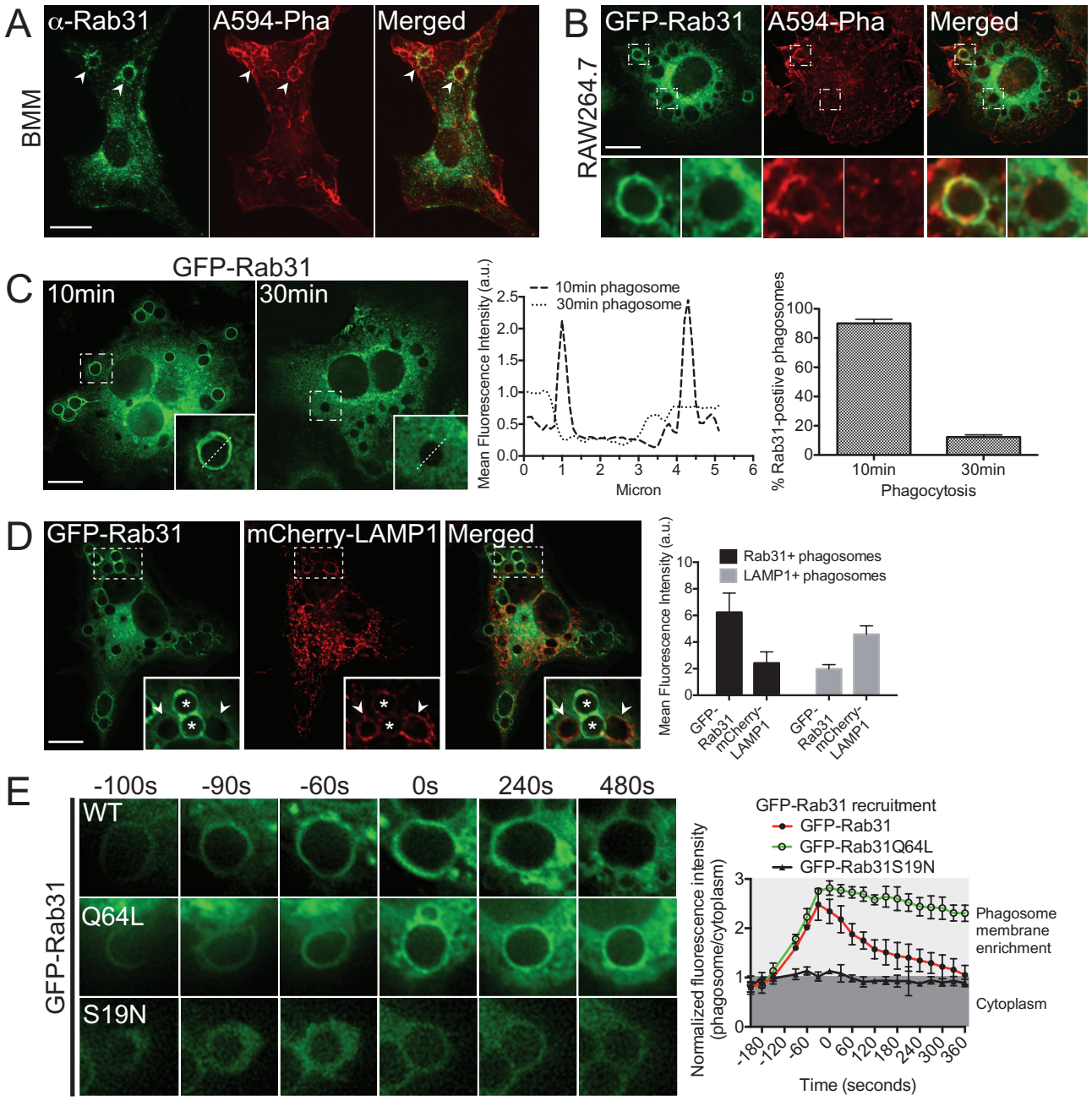

FIGURE 1: Early recruitment of Rab31 during FcγR-mediated phagocytosis. (A) Endogenous Rab31 in primary BMMs. Rab31 localized to F-actin–rich phagosomes. (B) GFP-Rab31 in transfected RAW 264.7 macrophages. GFP-Rab31 localizes to F-actin–rich phagosomes but is absent from phagosomes that have lost F-actin (inset). (C) Phagocytosis of IgG-beads within 10 and 30 min in GFP-Rab31–transfected RAW 264.7 cells. Inset, GFP-Rab31 contouring around a phagosome at 10 min but not 30 min. Line-scan fluorescence plot of the phagosomes comparing intensity of GFP-Rab31. Quantification of GFP-Rab31–positive phagosomes after 10 and 30 min of phagocytosis. Mean + SEM with $n = 30$ phagosomes from at least five cells. (D) RAW 264.7 cells cotransfected with GFP-Rab31 and mCherry-LAMP1. Inset, phagosomes mutually exclusive of Rab31 and LAMP1. Quantification of fluorescence intensity of GFP-Rab31 and mCherry-LAMP1 at the phagosomes. Mean + SEM with $n = 30$ phagosomes from at least five cells. (E) Live-cell imaging of GFP-Rab31, constitutively active Rab31 (GFP-Rab31Q64L), and dominant-negative Rab31 (GFP-Rab31S19N)–transfected macrophages ingesting IgG-sRBCs. The low fluorescence of GFP-Rab31S19N–transfected macrophages is enhanced to show phagocytosis of IgG-sRBCs. Right, quantification of fluorescence (phagosome/cytoplasm) from live cells, where $n = 5$ live phagocytic events. Scale bars, 10 μm.

(arrows). Remarkably, there was no labeling of GFP-Rab31 on the adjacent plasma membrane (arrowheads). This concurs with the live imaging, which showed separation of GFP-Rab31 on phagocytic cups compared with the surrounding plasma membrane domains enriched in $PI(4,5)P_2$ (Figure 2A). We can thus confirm that GFP-Rab31 is recruited to a closely circumscribed membrane domain at or after the point of phagocytic cup closure that is distinct from the plasma membrane.

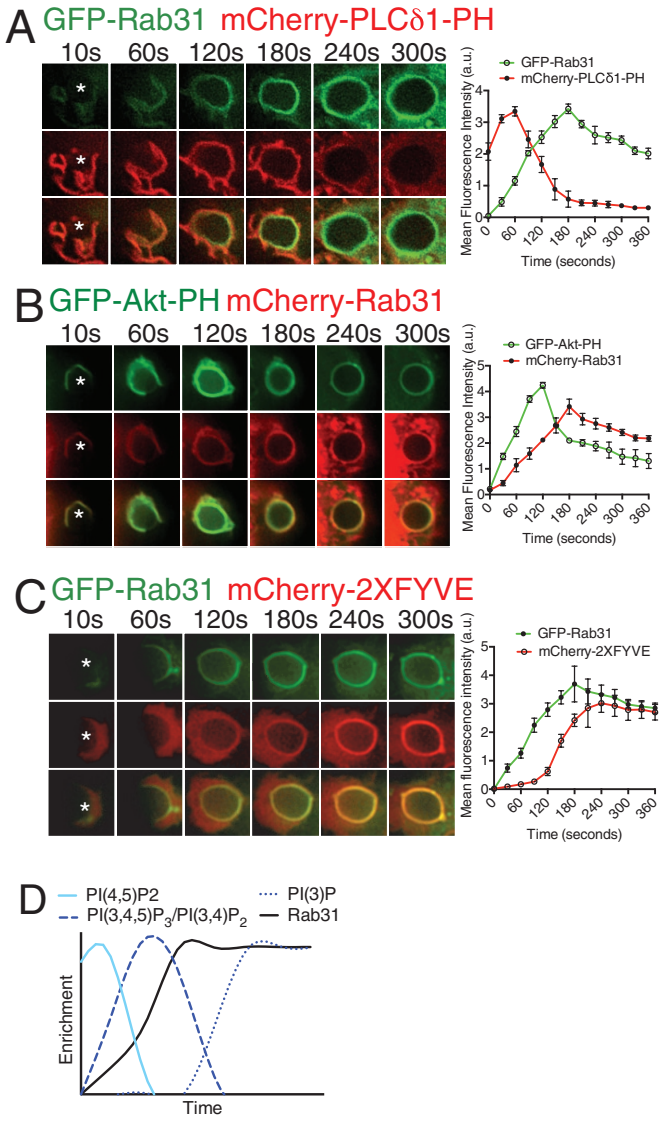

FIGURE 2: Rab31 is enriched on PI(4,5)P_2- and PI(3,4,5)P_2-positive phagocytic membranes and persists with PI(3)P. (A–C) Live-cell imaging of GFP/mCherry-Rab31 with GFP/mCherry-tagged phosphoinositide constructs, namely PLCδ1-PH, a (PI4,5)P_2 probe; Akt-PH, a PI(3,4,5)P_3/PI(3,4)P_2 probe; and 2XFYVE, a PI(3)P probe. Right, quantification of mean fluorescence intensity (MFI) on phagosomes. Mean + SEM with $n = 5$ live phagocytic events from three cells. (D) Graphical representation of enrichment of phosphoinositides with recruitment of Rab31 on phagosomes.

Rab31 is localized to a subset of PI(3)P membranes and is distinct from Rab5a on phagosomes

Rab31 is closely related to Rab5a, which was previously shown to be present on early phagosomes during bacteria- and FcγR-mediated phagocytosis (Vieira *et al.*, 2001; Bohdanowicz *et al.*, 2012; Seto *et al.*, 2011). We thus compared the distributions of Rab31 and Rab5a in macrophages (Figure 4). GFP-Rab5a was present on endosomes throughout the cells and on phagosomes near the cell surface (Figure 4A). In these locations, Rab5a overlapped frequently, as expected, with mCherry-2XFYVE on PI(3)P-positive membranes. In contrast, GFP-Rab31 was restricted to phagosomes, where it also overlapped with only mCherry-2XFYVE on phagosomes or the tubules emanating from them (Figure 4B). When cells were cotransfected with GFP-Rab31 and mCherry-Rab5a, the two Rabs only appeared together on early phagosomes; however, on close inspection, they can be seen to have different distributions on these phagosomes (Figure 4C). Whereas Rab31 exhibits its tight circumferential labeling, Rab5 is on vesicles and patches around the particle, consistent with its delivery via early endosome fusion. These results highlight the specificity of Rab31 for phagosomal, PI(3)P-enriched membranes in macrophages. Moreover, on the early phagosome, Rab31 is spatially distinct from Rab5a, foreshadowing different functions for each of these Rabs.

Rab31 recruits APPL2 as an effector on phagosomes in macrophages

Rab5a recruits the adaptor APPL1 as an effector, and the two participate in phospholipid modification and signaling during FcγR-mediated phagocytosis (Bohdanowicz *et al.*, 2012). A yeast two-hybrid study showed that Rab31 preferentially binds to the complementary adaptor APPL2 (King *et al.*, 2012), although, to our knowledge, APPL2 has not previously been examined in phagocytosis or in macrophages.

With this in mind, we performed an unbiased search for Rab31 effectors in extracts of activated macrophages, using glutathione *S*-transferase (GST)–Rab31 for pull downs. Bound proteins were eluted using the PreScission Protease cleavage method together with mass spectrometric analysis, and we previously showed that this approach can recover known Rab31 binding partners, such as EEA1 (Luo *et al.*, 2014a). In the experiments here, we highlight a protein band of ~75 kDa pulled down by GST-Rab31, for which five peptides matched the identity of APPL2 with 99% confidence and 10.2% coverage (Supplemental Figure S1A). A reverse pull down using GST-APPL2 as bait confirmed the binding of APPL2 to Rab31 in macrophages (Supplemental Figure S1B). Using purified APPL2 after cleavage of GST, together with GST-Rab31, we show direct binding of these two proteins. Moreover, APPL2 showed a preference for binding to GTP-loaded Rab31 compared with its GDP-bound form (Figure 5A). To examine the binding of APPL2 to GFP-Rab31 in cells, we performed immunoprecipitations on cell extracts. This confirms that APPL2 does bind to GFP-Rab31 in cells; moreover, if we compare this to GFP-Rab5a, there is a clear (threefold) preference of APPL2 for Rab31 (Figure 5B). Thus we show in macrophages that GTP-Rab31 can bind to APPL2 as an effector.

Endogenous APPL2 and GFP-APPL2 were examined in primary macrophages and in the RAW 264.7 cell line, and in both cases, APPL2 was immunolabeled in the cytoplasm, on cell surface ruffles, and on early, actin-rich phagosomes (Figure 5, C and D). This is the first evidence that APPL2 is associated with early phagosomes. The location of APPL2 on phagosomes is also consistent with that of Rab31 and offers a likely site for their interaction in cells as the major site of colocation.

Because APPL2 binds preferentially to GTP-Rab31, we coexpressed it with the constitutively active GFP-Rab31Q64L, which also colocalized on phagosomes. However, upon expression of the dominant-negative mutant of Rab31, there was significantly reduced phagosomal labeling of APPL2 (Figure 6A). A quantitative comparison revealed that both the wild-type and GTP-bound forms of Rab31 supported the localization of APPL2 to phagosomes, confirming this as the site for interaction of these proteins and suggesting that active Rab31 is required for APPL2 binding to phagosome membranes (Figure 6B). Membrane recruitment was further examined in live cells, where a time-lapse sequence and image analysis depicted Rab31 recruitment to the phagosome

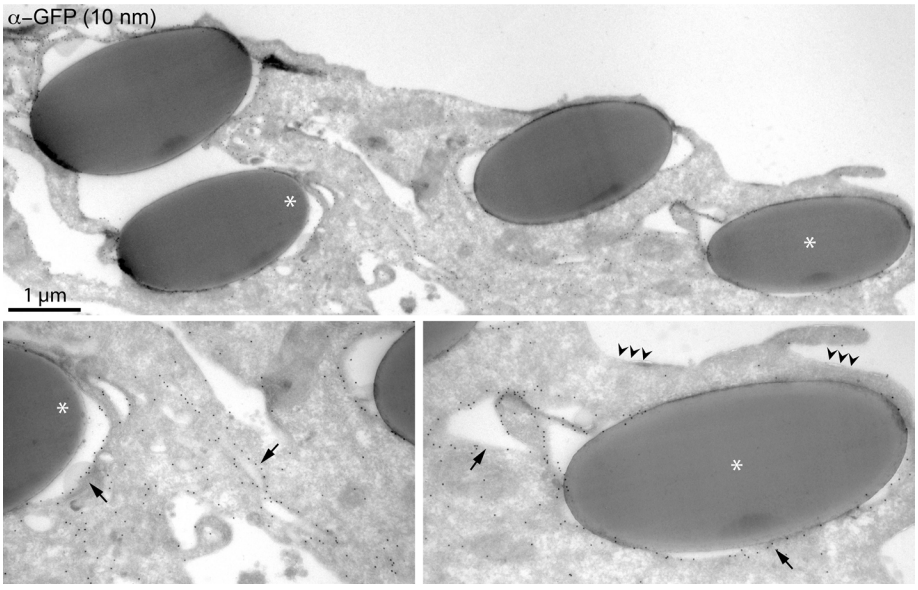

FIGURE 3: Rab31 is enriched on phagosomal membrane domains. Cryo-immunogold (10 nm) labeling of GFP-Rab31 in transfected macrophages. GFP-Rab31 is observed on phagosomal membranes upon 15 min of phagocytosis (arrows). The plasma membrane is depicted by arrowheads, and phagosomal membrane domains enriched with GFP-Rab31 are denoted by arrows. Insets, enlarged areas from phagosomes (asterisks) where GFP-Rab31 is concentrated. Scale bar, 1 μm.

occurring first, followed closely thereafter by APPL2 (Figure 6C). Once on the phagosomes, Rab31 and APPL2 were closely colocalized around the circumference.

Taken together, these results demonstrate that GTP-Rab31 and APPL2 bind to each other on early phagosomes during FcγR-mediated uptake. APPL2 is revealed as another new phagosome-associated protein. There appears to be preferential interaction of APPL2 with Rab31 in macrophages, and Rab31 contributes to or enhances recruitment of APPL2 to the phagosomes.

APPL2 and APPL1 define distinct membrane domains in macrophages

APPL2 and APPL1 are closely related isoforms. Rab31 binds to APPL2, but Rab5 binds to both APPL adaptors as Rab5 effectors (Miaczynska *et al.*, 2004). This prompted us to further compare both Rabs and both APPLs in macrophages (Figure 7). Membrane-bound GFP-APPL1 was widely distributed on small, punctate endosomes throughout the cells, and it was on surface ruffles and more weakly on early phagosomes (Figure 7A). This contrasts with the predominant and stronger labeling of mCherry-APPL2 on phagosomes and its general absence from endosomes (Figure 7A). Although both APPLs are bound to phagosomes, the merged and thresholded images in Figure 7A show that APPL1 is more punctate on phagosomes than the circumferential APPL2.

Enrichment of PI(3)P on endosomes has been shown to coincide with the displacement of APPL1 (Zoncu *et al.*, 2009), and this was observed on the endosomes and phagosomes in macrophages, when GFP-APPL1 and mCherry-2XFYVE were coexpressed and found largely in inverse patterns of membrane labeling. Phagosomes strongly labeled with mCherry-2XFYVE had only weak APPL1 labeling (Figure 7B). In live cells, APPL1 was found around very early phagosomes, disappearing at 240 s when mCherry-2XFYVE staining was increasing, and again their inverse relationship is shown by the normalized intensity plots (Figure 7C). In contrast, APPL2 colocalized strongly on phagosomes throughout the cell with mCherry-2XFYVE (but notably not on PI(3)P-enriched endosomes; Figure 7D), and in live cells, APPL2 was recruited to phagosomes before mCherry-2XFYVE but then persisted with PI(3)P (Figure 7E). This last result showed that APPL2 closely mirrored the recruitment and persistence of Rab31 on PI(3)P domains during phagocytosis. Based on their staining patterns (Figure 7A) and the fluorescence plots of their recruitment in live cells (Figure 7, C and E), we conclude that APPL1 and APPL2 are spatially and temporally distinct on phagosomes, consistent with their recruitment by different Rabs. APPL2 was not displaced during PI(3)P enrichment and was retained on phagosomes for significantly longer than APPL1. Coimaging and quantification also revealed that APPL1 is aligned more closely with the distribution of Rab5a, whereas APPL2 colocalized with Rab31 (Figure 7F). Thus, in macrophages, there is a spatial distinction between these two sets of Rabs and adaptors. This positions the APPL adaptors to function individually at this location.

Depletion of Rab31 or APPL2 delays cup closure and impairs FcγR-mediated phagocytosis

Given the recruitment of both Rab31 and APPL2 to early-stage phagosomes, we examined their possible roles in the phagocytic process by depleting cells of these proteins. Specific small interfering RNAs (siRNAs) produced a 60% decrease in Rab31 mRNA levels (Figure 8A), and those targeting APPL2 reduced expression of APPL2 protein below detectable levels (Figure 8B). Macrophages allowed to phagocytose IgG-beads were analyzed using a quantitative image-based assay that measures the proportion of beads attached to the cells (before phagocytosis) and those that have been fully internalized into closed phagosomes (after phagocytosis; Yeo *et al.*, 2013). Under these conditions, in untreated cells or siRNA controls, ~50% of the beads are phagocytosed at 10 min. Knockdown of Rab31 or APPL2 significantly decreased the proportion of internalized beads, with a concomitant increase in the beads remaining surface attached in each case (Figure 8C and Supplemental Figure S2). Thus loss of either Rab31 or APPL2 results in less efficient internalization of beads into closed phagosomes, implying that these proteins both have roles in the early phagocytic process.

Phagocytic cup closure is linked to phosphoinositide transition, where $PI(3,4,5)P_3$ is important for sealing of phagocytic cups (Araki *et al.*, 2003). We thus examined phagocytic cup closure in more detail in control and Rab31- and APPL2-depleted cells expressing the $PI(3,4,5)P_3$ probe GFP-Akt-PH. Live-cell imaging during attachment and engulfment of IgG-sRBCs revealed the membrane recruitment of the GFP-Akt-PH probe (15 s) after particle contact, upon particle contact (arrowhead, peak), and during phagocytic cup closure (asterisks) in representative time-lapse movies in control cells (Figure 8D). However, depletion of either Rab31 or APPL2 delayed this process. Less GFP-Akt-PH accumulated under the attached particle, delaying the process of engulfment and cup closure by a full 2 min. In addition, GFP-Akt-PH then quickly dissociated (by 420 s) after phagosome closure in Rab31- or APPL2-depleted cells, and this is reflected in the quantification of GFP-Akt-PH fluorescence throughout phagocytosis.

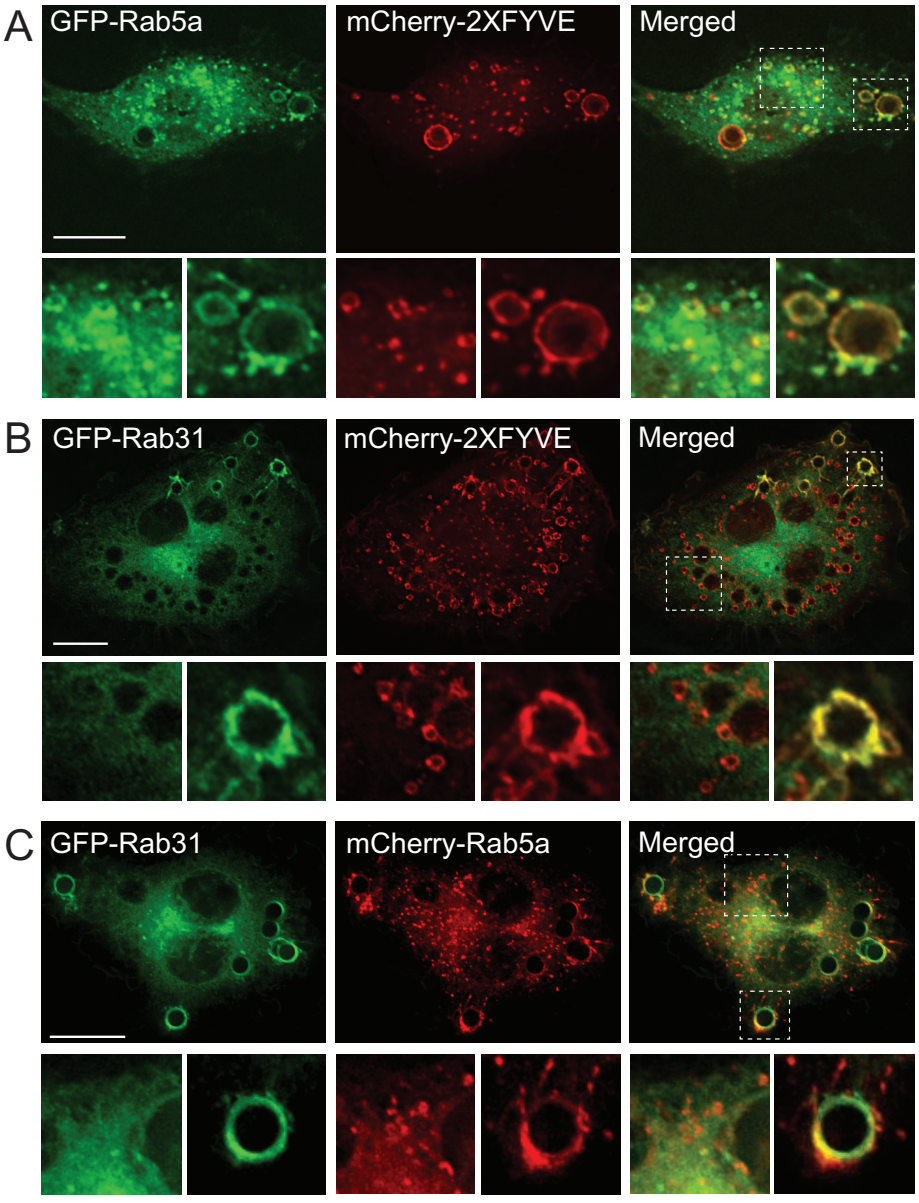

FIGURE 4: Rab31 associates with PI(3)P-containing phagosomes but not with other PI(3)P endosomes. RAW 264.7 macrophages coexpressing combinations of GFP/mCherry-tagged Rab31, Rab5a, and 2XFYVE were exposed to IgG-beads and fixed after 10 min of phagocytosis. (A) Coexpression of GFP-Rab5a and mCherry-2XFYVE showing colocalization of Rab5a and PI(3)P in endosomes and phagosomes in macrophages. (B) Coexpression of GFP-Rab31 and mCherry-2XFYVE showing colocalization of Rab31 and PI(3)P at phagosomes but not other PI(3)P endosomes. (C) Coexpression of GFP-Rab31 and mCherry-Rab5a showing limited colocalization on phagosomes and other PI(3)P endosomes. Scale bars, 10 μm.

These findings together implicate Rab31-recruited APPL2 as a key mediator of phagocytosis, possibly through the regulation of phosphoinositide transitions at the point of phagocytic cup formation. Because $PI(3,4,5)P_3$ is a platform for signaling molecules, we next examined signaling downstream of FcγR activation.

APPL2 enhances Akt and decreases mitogen-activated protein kinase p38 signaling during FcγR activation

$PI(3,4,5)P_3$ and $PI(3,4)P_2$ are important for the recruitment of PDK-1 and Akt to the inner leaflet of the plasma membrane, where PDK-1 phosphorylates and activates the serine/threonine-specific kinase Akt (Currie *et al.*, 1999). We examined the recruitment of full-length Akt to phagosomes in both control and APPL2-depleted cells transiently expressing GFP-Akt. In control cells, the normally cytoplasmic GFP-Akt was enriched at the membrane at the base of surface-attached IgG-sRBCs and around phagocytic cups during their subsequent engulfment before dissipating at later times (beyond 60 s; Figure 9A). In cells depleted of APPL2, there was a marked difference, with a significant reduction in recruitment of GFP-Akt to these membrane domains during attachment or phagocytosis; instead, diffuse labeling of GFP-Akt in the surrounding cytoplasm predominated (Figure 9A). The fluorescence plot shows that control cells have at least a twofold increase (above cytoplasmic levels) of GFP-Akt on the phagosome at a time coinciding with enrichment of $PI(3,4,5)P_3$, just after cup closure. In APPL2-depleted cells, the fluorescence of GFP-Akt detected on the phagosome was barely above cytoplasmic levels throughout this time course. The reduced recruitment of Akt is thus in keeping with reduced levels of $PI(3,4,5)P_3$ and a reduction in phosphorylated Akt during FcγR signaling.

FcγR activation leads to phosphorylation of major signaling kinases, including the serine/threonine-specific protein kinase Akt and p38 mitogen-activated protein kinase (p38 MAPK). To see whether APPL2 directly affects FcγR-mediated signaling, we examined the phosphorylation of this kinase in control and APPL2-knockdown cells. In cells depleted of APPL2, there was a 50% reduction in the phosphorylation of Akt (p-Akt) and a simultaneous increase in the phosphorylation of p38 (p-p38) by twofold at 30 and 60 min after FcγR stimulation (Figure 9B). As an additional approach, we measured signaling in cells overexpressing APPL2 (Figure 9C). This shows the opposite trend, with an increase in p-Akt and decreased p-p38 in overexpressing cells, nicely confirming the previous result. We thus conclude that APPL2 increases Akt and decreases p38 signaling from activated FcγR. Of interest, a previous study showed that knockdown of APPL1 in macrophages produced the opposite effect, increasing Akt and decreasing p38 signaling during phagocytosis (Bohdanowicz *et al.*, 2012). For comparison, in Figure 9D, we overexpressed APPL1 and found a resulting decrease in p-Akt and increase in p-p38, confirming the knockdown signaling phenotype of APPL1 reported by Bohdanowicz *et al.* (2012).

Taken together, the results show that APPL2 modulates FcγR signaling and does so in an opposing manner to APPL1.

DISCUSSION

Rab GTPases regulate a multitude of cell functions by temporally recruiting specific effector molecules to membrane domains. The

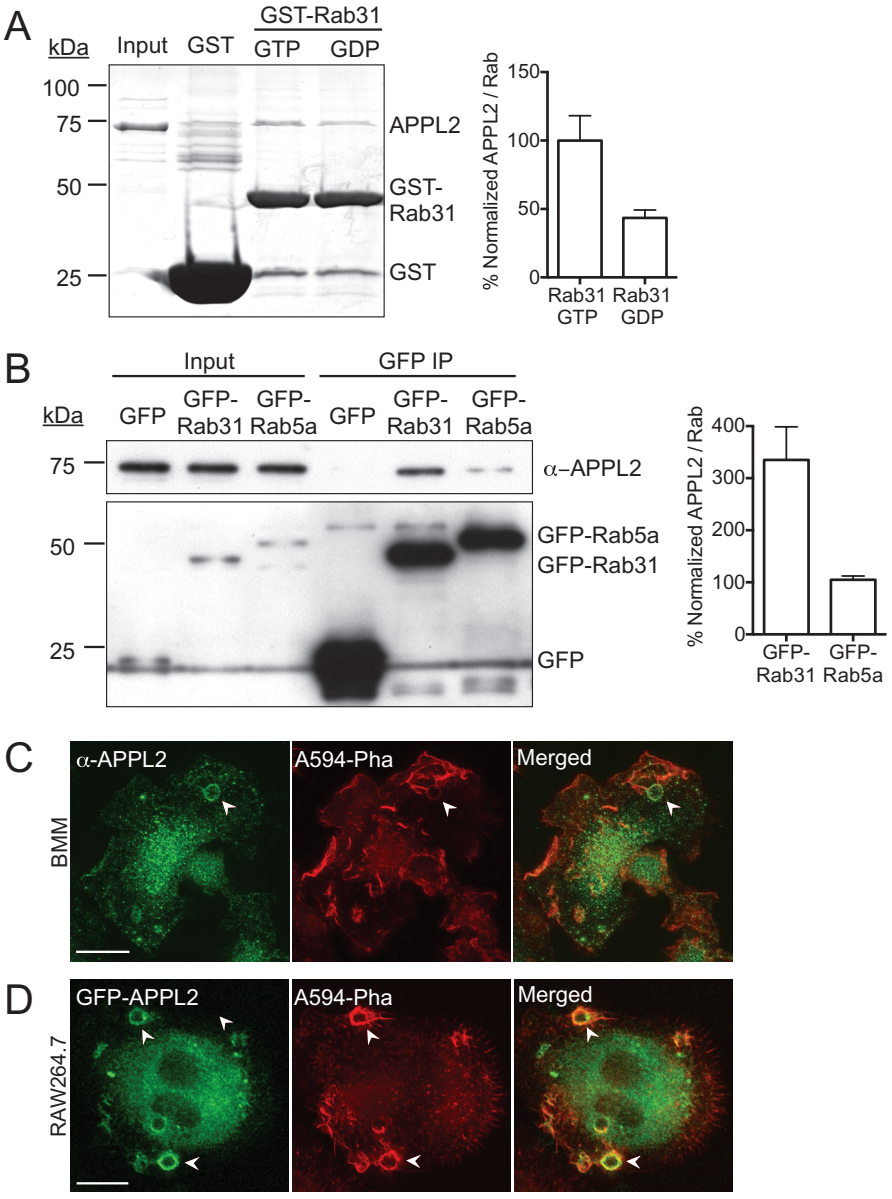

FIGURE 5: APPL2 is a Rab31 effector and is recruited to membrane ruffles and phagosomes in macrophages. (A) Direct binding of purified APPL2 to GST-Rab31. Nucleotide exchange using GTP or GDP was performed on purified GST-Rab31, and cleaved APPL2 was incubated with GTP- or GDP-bound GST-Rab31. GST alone was used as a control, and purified cleaved APPL2 was used as input. Right, quantification of APPL2 binding to GTP/GDP-bound Rab31. Quantification was performed by densitometric analysis of Coomasie blue–stained gels normalized to GST control. (B) Coimmunoprecipitation of APPL2 by GFP-Rab31 and GFP-Rab5a in lysates from transfected RAW 264.7 cells. GFP transfection alone was used as a control. Quantification was performed by densitometric analysis of Western blots normalized to GFP control. (C) Endogenous labeling of APPL2 in BMMs after ingestion of IgG-beads. F-actin– rich structures were depicted with Alexa 594–phalloidin. (D) RAW 264.7 macrophages transfected with GFP-APPL2 during phagocytosis of IgG-beads, showing recruitment of APPL2 to phagocytic structures depicted by Alexa 594–phalloidin labeling. Mean + SEM. Scale bar, 10 μm.

signaling adaptors APPL1 and APPL2 are known effectors of the Rab5 subfamily on a subset of signaling endosomes derived from the cell surface (Miaczynska *et al.*, 2004; Urbanska *et al.*, 2011; King *et al.*, 2012). These adaptors typically function as scaffolds for receptors and signaling molecules, and the Rab-APPL complexes therefore directly drive signaling for cell growth, survival, and apoptosis in response to various growth stimuli (Miaczynska *et al.*, 2004; Schenck *et al.*, 2008; Wang *et al.*, 2009, 2012; Pyrzynska *et al.*, 2013). Here we show recruitment of APPL1 and APPL2 by Rab5a and Rab31, respectively, to distinct membrane subdomains during phagocytosis. Moreover, we find that in macrophages, Rab31 and APPL2 are largely confined to phagosomal membranes, where they have demonstrable roles in phagosome closure and FcγR signaling.

Rabs, among other cytoskeletal and membrane components, are recruited temporally throughout the process of phagocytosis. Our results establish a new predominant location for Rab31 in macrophages on early phagosomes, in contrast to its association with post-Golgi trafficking pathways reported in other cell types (Rodriguez-Gabin *et al.*, 2001; Lodhi *et al.*, 2007). Rab31 is recruited directly from the cytoplasm to a tightly defined membrane domain created by the initiation of phagocytosis, which was evident at both light microscopic and ultrastructural levels. Distinct phosphoinositide species are sequentially enriched during phagocytosis for phagosome formation and maturation, and this has been elegantly portrayed using a variety of phosphoinositide probes (Grinstein, 2010). Using a similar approach, we were able to pinpoint the initial recruitment of Rab31 to newly forming phagocytic cups at a stage in between $PI(4,5)P_2$ and PI(3)P, and its persistence after conversion to PI(3)P, during maturation of phagosomes. The initial recruitment of Rab31 coincided with enrichment of the Akt-PH probe, denoting the production of the signaling phosphoinositide $PI(3,4,5)P_3$. These membrane domains associated with early-stage phagocytosis share dual roles in particle engulfment and receptor signaling (Flannagan *et al.*, 2010; Jaumouillé *et al.*, 2014). The location and timing of Rab31 recruitment are therefore suggestive of potential modulatory roles in phosphoinositide-dependent functions during phagocytic cup closure and FcγR clustering and signaling. and the identity of appropriate effectors is then critical.

In this study, an unbiased screen revealed and confirmed the signaling adaptor APPL2 as a major effector binding to Rab31-GTP in macrophages. This concurred with the binding of APPL2 to Rab31 found previously by yeast two-hybrid screening (King *et al.*, 2012). Both studies also show that APPL2 has a preference for binding to Rab31 over Rab5a. The present data indicate higher binding preference of APPL2 to GFP-Rab31 compared with Rab5a, and our localization studies show that APPL2 colocalizes with Rab31 more abundantly than with Rab5a. APPL functions have generally been attributed to Rab5 (Miaczynska *et al.*, 2004; Zhu *et al.*, 2007; Bohdanowicz *et al.*, 2012; King *et al.*, 2012), but closer examination of distinct functions for Rab31 and APPL2

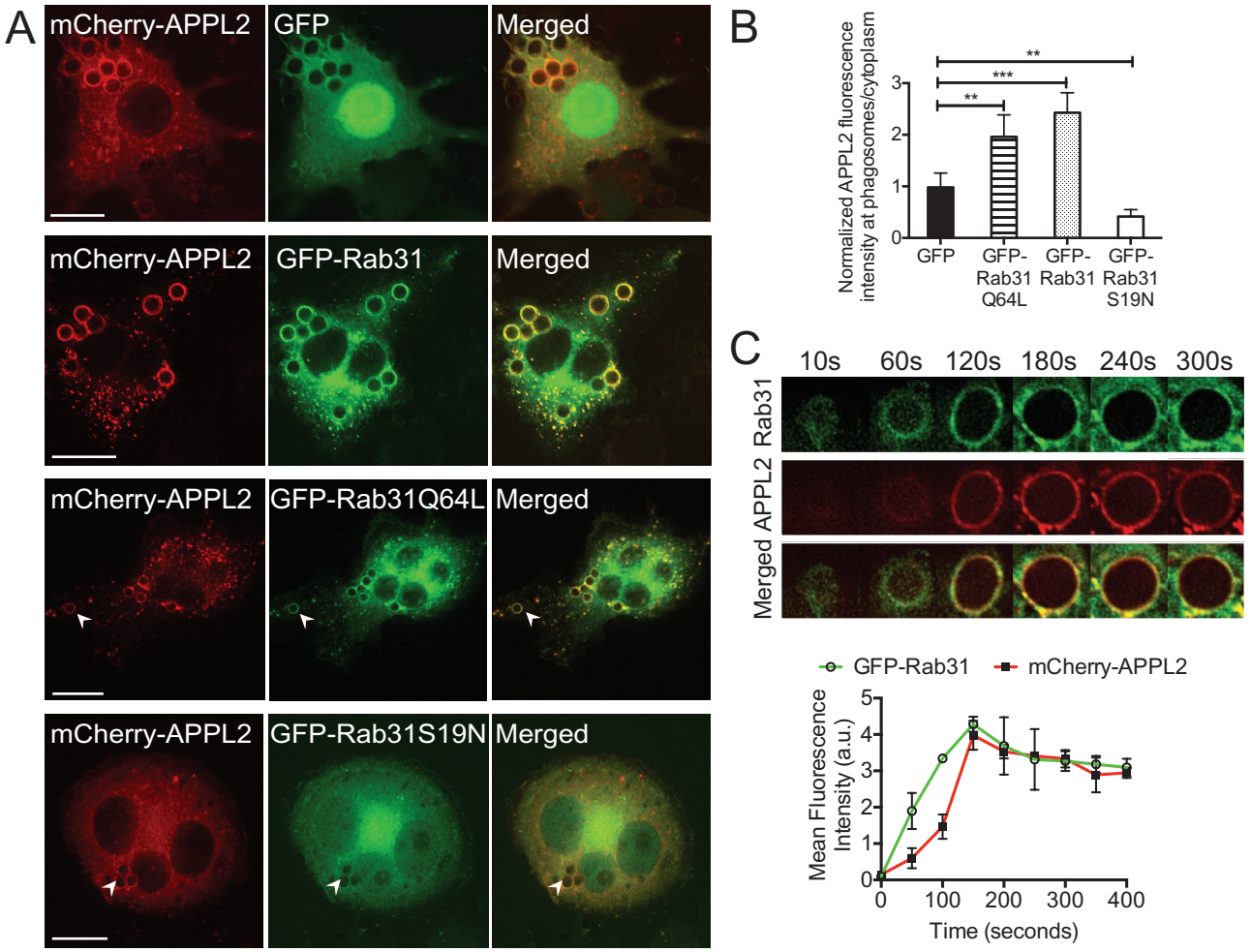

FIGURE 6: Rab31 recruits APPL2 onto endosomes and phagosomes. (A) Cotransfection of mCherry-APPL2 with GFP control, GFP-Rab31, constitutively active mutant of GFP-Rab31 (GFP-Rab31Q64L), and dominant-negative mutant of GFP-Rab31 (GFP-Rab31S19N) during phagocytosis of IgG beads after 15 min. (B) Quantification of mCherry-APPL2 fluorescence from A. Mean + SEM with $n = 30$ phagosomes from at least five cells. (C) Live-cell imaging of a macrophage cotransfected with GFP-Rab31 and mCherry-APPL2 during phagocytosis of IgG-sRBCs. Representative time slices are chosen to depict the spectrum of enrichment of both proteins at the phagosomes. Quantification of live-cell imaging from cotransfected cells. Mean + SEM, with $n = 5$ live phagocytic events from three cells.

within these cell systems may now be warranted based on our findings. Several lines of evidence in the present study show that Rab31 and APPL2 are colocalized as a functional pair on phagosomes, whereas Rab5 and APPL1 are colocalized with each other on distinct subdomains within phagosomes and elsewhere in the cells. APPLs, most particularly APPL1, typically localize to signaling endosomes, which are characterized as precursors to early endosomes (Miaczynska *et al.*, 2004; Zoncu *et al.*, 2009). Endosomal acquisition of PI(3)P and transition from signaling to early endosomes normally induces dissociation of APPL1, corresponding to the termination of receptor signaling (Zoncu *et al.*, 2009). However, during phagocytosis, we show that recruitment of APPL2, but not APPL1, to phagosomes was unaffected by phagosomal acquisition of PI(3)P, suggesting yet another disparity between the two APPL proteins in this context. Thus APPL2 is distinguished from APPL1 in macrophages by having Rab31 as a direct, preferential binding partner and by its distinct temporal recruitment to membrane subdomains during phagocytosis.

APPL2 and Rab31 depletion demonstrated a functional requirement for both proteins for efficient phagocytic uptake of IgG-coated particles. Depleting APPL2 arrested phagocytic cups at a semi-formed stage before closure. Furthermore, analysis of phosphoinositides in live cells showed delayed production of $PI(3,4,5)P_3$, as indicated by labeling with the Akt probe in Rab31- and APPL2-depleted macrophages. Abortive phagocytosis as a result of reduced $PI(3,4,5)P_3$ at the phagocytic cups correlates with the effects of the phosphatidylinositol 3-kinase (PI3K) inhibitor wortmannin, which blocks phagocytosis at the cup closure stage (Cox *et al.*, 1999). By creating a similar phenotype, the results of depleting APPL2 suggest a potential role for this adaptor in regulating or recruiting a PI3K for cup closure. Multiple class 1A PI3K isoforms (Leverrier *et al.*, 2003; Lee *et al.*, 2007; Tamura *et al.*, 2009) have been associated with phagosomes. We also recently showed that Rab8a recruits a class 1B PI3K to the ruffles that would normally precede phagosomes (Luo *et al.*, 2014b) in activated macrophages. Of interest, APPL1 depletion reportedly does not affect phagocytic cup closure (Bohdanowicz *et al.*, 2012). This is in spite of finding that APPL1 can interact with the p110α and β subunits of class 1A PI3K in other circumstances (Mitsuuchi *et al.*, 1999; Tan *et al.*, 2010a; Wang *et al.*, 2012).

The early phagocytic cup is also a signaling center mediating multiparametric downstream signaling cascades (Swanson and Hoppe, 2004), many of which depend on $PI(3,4,5)P_3$, for instance, for recruiting signaling kinases such as Akt. Therefore our studies

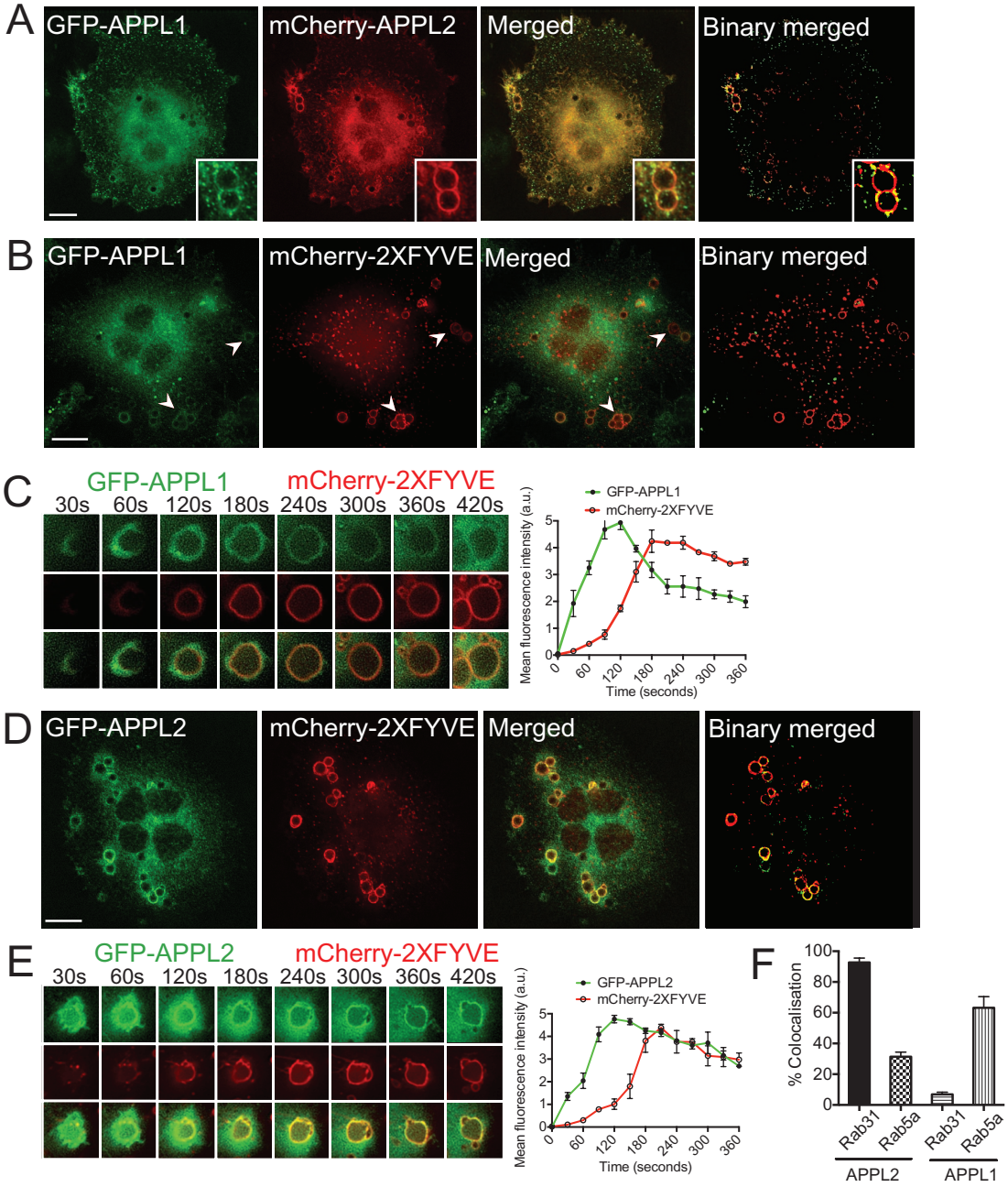

FIGURE 7: APPL2 is spatiotemporally distinct from APPL1 on phagosomes. (A) GFP-APPL1 and mCherry-APPL2 localization in cotransfected macrophages during phagocytosis of IgG beads. Inset, segregation of GFP-APPL1 and mCherry-APPL2 on phagosomes. (B) Cotransfections of GFP-APPL1 with mCherry-2XFYVE during phagocytosis in macrophages after 15 min to achieve enrichment of PI(3)P on phagosomes. (C) Live-cell imaging of cotransfected cells upon ingestion of IgG-sRBCs; right, fluorescence plot of GFP-APPL1 and mCherry-2XFYVE on the phagosome. (D) Cotransfections of GFP-APPL2 with mCherry-2XFYVE during phagocytosis in macrophages after 15 min to achieve enrichment of PI(3)P on phagosomes. (E) Live-cell imaging of cotransfected cells upon ingestion of IgG-sRBCs; right, fluorescence plot of GFP-APPL2 and mCherry-2XFYVE on the phagosome. Data in C and E are represented as mean + SEM, with $n = 5$ live phagocytic events from three cells. (F) Macrophages coexpressing combinations of mCherry-APPL2/GFP-Rab5a, GFP-APPL1/mCherry-Rab5a, and GFP-APPL1/mCherry-Rab31. Quantification of colocalization. Mean + SEM where $n = 10$ cells. Scale bars, 10 μm.

also examined FcγR-mediated signaling after depletion of APPL2. Consistent with a decreased level of PI(3,4,5)P_3, APPL2 depletion resulted in decreased phosphorylation of Akt. Conversely, overexpressing APPL2 increased Akt phosphorylation, indicating that APPL2 normally serves to enhance signaling via the PI3K/Akt pathway. Another notable effect of APPL2 depletion and overexpression was on p38 phosphorylation in the MAPK pathway. These results together strongly suggest that APPL2 normally serves to reduce p38 MAPK signaling and to mediate signaling characteristic of an Akt-mediated prosurvival response in activated macrophages. Our findings point to APPL2 regulation of macrophage survival in immune responses, in line with the literature showing that the Akt and p38 MAPK signaling pathways are differentially regulated during cell survival and apoptosis in response to various stimuli

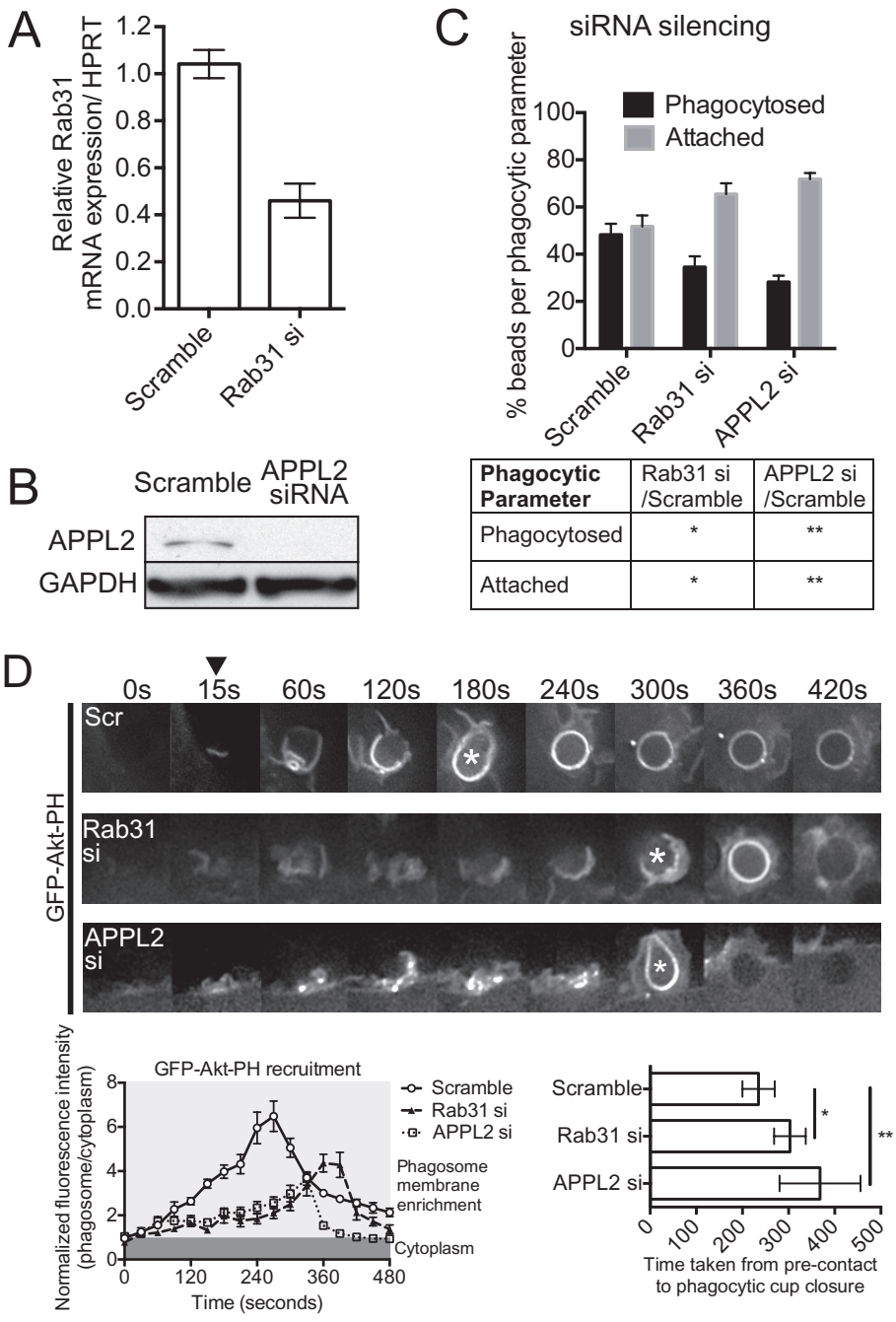

Phagocytic Parameter	Rab31 si /Scramble	APPL2 si /Scramble
Phagocytosed	*	**
Attached	*	**

FIGURE 8: Depletion of Rab31 and APPL2 attenuates phagocytosis of IgG-beads. (A) Real-time PCR detection of RAW 264.7 macrophages depleted with siRNAs against Rab31. A nontargeting, scrambled siRNA was used as a control. (B) Western blot detection of APPL2 in macrophages depleted with siRNA against APPL2. Similar nontargeting scrambled siRNA was used as a control. (C) Quantification of phagocytosis in Rab31 and APPL2 siRNA-depleted cells. Results are represented as the percentage change compared with scrambled control and depicted as mean + SEM with $n = 15$ fields of view from three experiments. (D) RAW 264.7 cells were treated with scrambled or APPL2 siRNA for 48 h, and GFP-Akt-PH was transfected into cells 24 h before experiments. Their recruitment to IgG-sRBC phagosomes was measured over time throughout live-cell imaging of phagocytosis. IgG-sRBCs were observed to attach to cells upon 15 s (black arrowhead), as seen by the accumulation of GFP-Akt-PH at the base of the phagocytic cups, and closure of the phagocytic cups is shown (asterisks). The fluorescence intensity plot of GFP-Akt-PH and graph of time taken for phagocytic cup closure are shown below comparing control and Rab31- and APPL2-depleted cells. Mean + SEM with $n = 5$ live phagocytic events from three cells.

(Gratton *et al.*, 2001; Liao and Hung, 2003; Rane *et al.*, 2010).

Remarkably, APPL1 appears to have the opposite effect to APPL2 in FcγR-mediated signaling. APPL1 depletion (Bohdanowicz *et al.*, 2012) or its overexpression (in the present study) indicate that APPL1 functions to reduce Akt signaling and increase p38 MAPK signaling. Rab5a is required for the recruitment of APPL1 to early phagosomes (Bohdanowicz *et al.*, 2012), and our present biochemical and localization results are consistent with independent localization and functions for Rab5a/APPL1 versus Rab31/APPL2. Rab5a/APPL1 has been suggested to function in reducing Akt signaling from FcγR by recruiting the inositol 5-phosphatase OCRL (Bohdanowicz *et al.*, 2012). Indeed, the inositol 5-phosphatases OCRL and INPP5B are known binding partners of APPL1 but not of APPL2 (Erdmann *et al.*, 2007). Rab5, APPL1, OCRL, and INPP5B can limit $PI(4,5)P_2$ on phagosome membranes and therefore limit the production of $PI(3,4,5)P_3$, for Akt signaling (Loovers *et al.*, 2007; Bohdanowicz *et al.*, 2012; Marion *et al.*, 2012). In contrast, our data show that APPL2 enhances the presence of $PI(3,4,5)P_3$ and enhances Akt signaling. The most obvious, but not only possible, mechanism would be for APPL2 to recruit a PI3K. As noted, this PI3K would function for cup closure and signaling. At least two PI3K isoforms, PI3Kδ and PI3Kγ, are known to be involved in signaling from TLRs during pathogen detection, but their involvement in FcγR signaling has not been addressed (Aksoy *et al.*, 2012; Luo *et al.*, 2014b). It is not known whether these or any other PI3K subunits are recruited or regulated by APPL2, and this remains to be elucidated in future studies.

Our results also reveal a new example of APPLs 1 and 2 working in disparate roles. The fact that APPL proteins can form homodimers and heterodimers perpetuated the view that they likely have redundant functions (Chial *et al.*, 2008, 2010; Urbanska *et al.*, 2011). However, other studies also showed that APPL1 and 2 can function independently (Wang *et al.*, 2009; Pyrzynska *et al.*, 2013). Knockdown of APPL2 in $APPL1^{-/-}$ murine fibroblasts showed that both APPLs differentially regulated epidermal growth factor and hepatocyte growth factor signaling pathways (Chial *et al.*, 2010; Tan *et al.*, 2010b). Another report showed that both APPL proteins have opposing effects in adiponectin- and insulin-mediated signaling, where APPL2 competitively inhibits APPL1 binding to the receptors and downregulates signaling (Wang *et al.*, 2009). Our

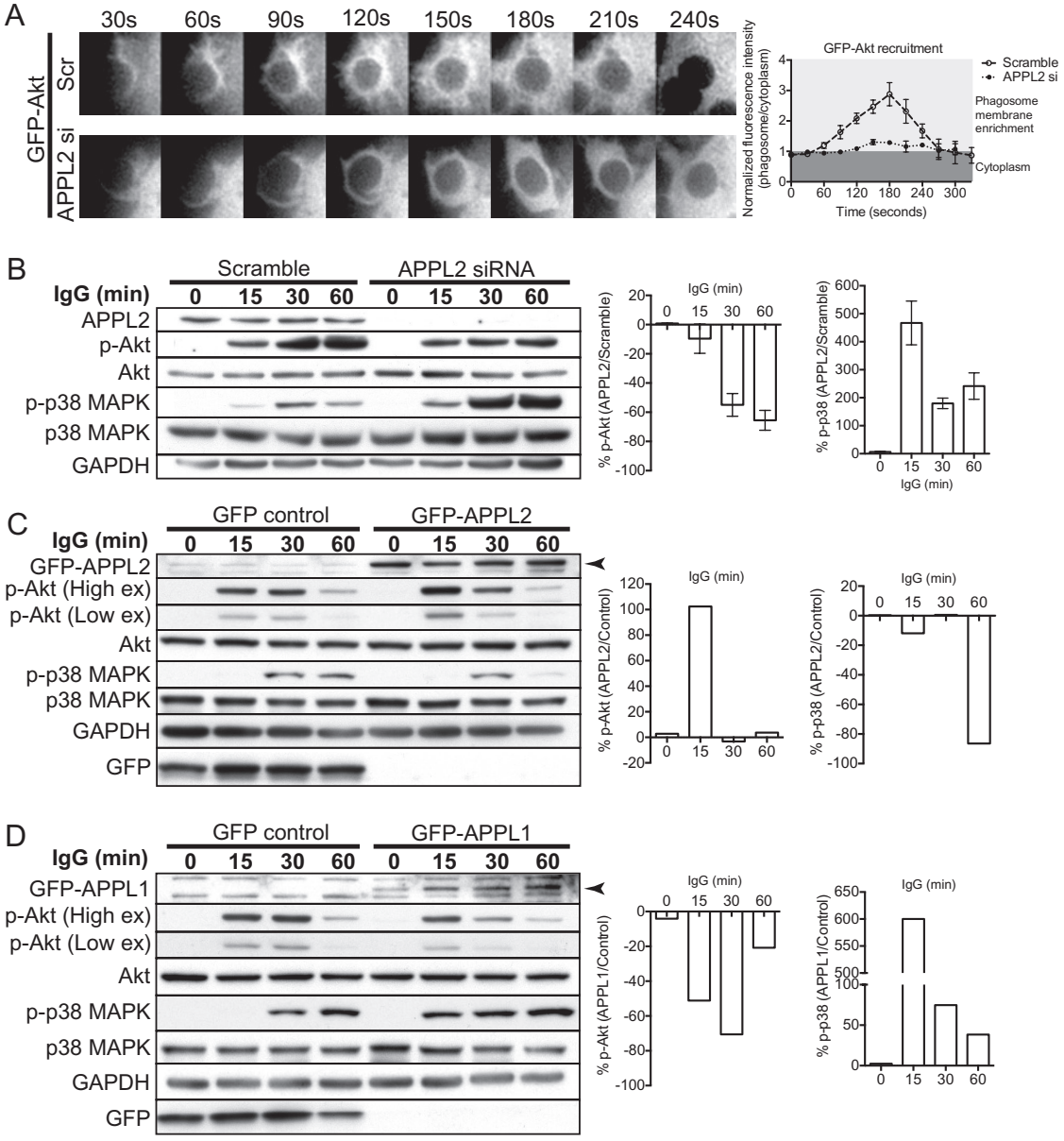

FIGURE 9: APPL2 enhances FcγR-mediated Akt signaling. (A) RAW 264.7 cells were treated with scrambled or APPL2 siRNA for 48 h, and GFP-Akt was transfected into cells 24 h before experiments. Their recruitment to IgG-sRBC phagosomes was measured over time throughout live-cell imaging of phagocytosis. Right, fluorescence intensity plot of GFP-Akt comparing control and APPL2-depleted cells. Mean ± SEM with $n = 5$ live phagocytic events from three cells. (B) Western blot detection of Akt and p38 MAP kinase signaling in a time course of phagocytosis in APPL2-depleted cells. Scrambled or APPL2 siRNA–treated RAW 264.7 macrophages were allowed to phagocytose IgG-sRBCs for 15, 30, and 60 min and then lysed and harvested for Western blotting. APPL2 was almost completely eliminated in APPL2 siRNA–treated cells. p-Akt (Ser-473) and p-p38 MAPK (Thr-180/Tyr-182), Akt, and p38 MAPK were probed for Western detection, and GAPDH was used as a loading control. Right, corresponding quantification of p-Akt and p-p38 MAPK levels shown as APPL2-depleted cells relative to scrambled control cells. Mean ± SEM with $n = 3$. (C, D) RAW264.7 macrophages overexpressing GFP-APPL2 and GFP-APPL1 were exposed to a similar time course of phagocytosis (0, 15, 30, and 60 min), and lysates were probed for GFP, p-Akt, p-p38 MAPK, Akt, p38 MAPK, and GAPDH.

results showing distinct locations and functions for APPL1 and APPL2 in macrophages further entrenches the concept that these adaptors have separate, modulatory roles. These Rab/adaptor complexes are introduced as mediators with potentially crucial roles in biasing receptor signaling to determine the outcome of immune activation in innate immunity. Their roles highlight the early phagosome as a parallel receptor signaling platform that is reminiscent of, but distinct from, the Rab-APPL signaling endosomes involved in other stimulus-coupled pathways and other cell types (Miaczynska *et al.*, 2004; Nechamen *et al.*, 2007; Rashid *et al.*, 2009; Wang *et al.*, 2009, 2012; Zoncu *et al.*, 2009; Bohdanowicz *et al.*, 2012).

In conclusion, we present Rab31 and its effector APPL2 as new players in the regulation of FcγR-mediated phagosome formation and PI3K/Akt prosurvival signaling in macrophages. In this setting, Rab31 and APPL2 are poised to act as components of a Rab cascade that drives phagocytosis and signaling.

MATERIALS AND METHODS

Antibodies and reagents

Rab31 antibody was purchased from Abnova and APPL2 antibody from Abcam. Phospho-Akt (Ser-473), phosphoxp38 MAPK (Thr-180/Tyr-182), and Rab5 antibodies used in this study were purchased from Cell Signaling Technology (Beverly, MA). GST antibody was purchased from Invitrogen (Mulgrave, VIC, Australia). Anti–glyceraldehyde-3-phosphate dehydrogenase (GAPDH) was purchased from Trevigen (Gaithersburg, MD). LAMP1 antibody was purchased from BD Biosciences (San Jose, CA). Alexa Fluor 488–, 594–, and 647–conjugated secondary antibodies were purchased from Molecular Probes/Invitrogen (Eugene, OR). Horseradish peroxidase–conjugated goat anti-mouse and anti-rabbit antibodies were obtained from Zymed (San Francisco, CA). Bacterial lipopolysaccharide (LPS), purified from *Salmonella enterica* serotype Minnesota Re 595, was purchased from Sigma-Aldrich (Castle Hill, NSW, Australia). For phagocytosis, human IgG (Invitrogen) was conjugated to 3-µm latex beads (Sigma-Aldrich) and sheep red blood cells (Australian Ethical Biologicals, Coburg, Australia) was conjugated with rabbit anti-sheep IgG (Sigma-Aldrich). All other chemicals and reagents were from Sigma-Aldrich.

Constructs

Mouse GFP-tagged Rab5a and Rab31 constructs were kindly provided by Mitsunori Fukuda (Tohoku University, Sendai, Japan) and were subcloned into the pmCherry-C1 vector (Clontech, Mountain View, CA). The mouse APPL1 and APPL2 cDNAs were obtained from the Facility for Life Science Automation (LISA) at the Institute for Molecular Bioscience (IMB). APPL2 and APPL1 were cloned into pEGFP-C1 and pm-Cherry-C1 vectors (Clontech). Rab31 and APPL2 were also subcloned into pGEX-6P-1 and expressed in *Escherichia coli* as previously described (Collins *et al.*, 2005). Phosphoinositide probes (GFP-PLCδ1-PH, GFP-Akt-PH, and mCherry-2XFYVE) were kindly provided by Frederic Meunier (University of Queensland, Brisbane, Australia). GFP-PLCδ1-PH and GFP-Akt-PH were subcloned into pmCherry-C1 vectors. GFP-Akt was kindly provided by Julian Downward (Addgene plasmid 39531; Watton and Downward, 1999).

siRNA knockdown and cell culture

BMMs were obtained by ex vivo differentiation of bone marrow cells collected from mouse femurs or tibias. Cells were differentiated for 7 d in complete RPMI 1640 medium (Lonza, Mount Waverly, VIC, Australia) supplemented with 20 U/ml penicillin, 20 µg/ml streptomycin, and 100 ng/ml purified recombinant macrophage colony-stimulating factor-1 (Hume and Gordon, 1982; Tushinski *et al.*, 1982). The mouse RAW 264.7 macrophage cell line was cultured in RPMI medium supplemented with 10% heat-inactivated fetal calf serum (Thermo Trace) and 2 mM L-glutamine (Invitrogen) in humidified 5% CO_2 at 37°C as previously described (Shurety *et al.*, 2000). For transient expression of cDNA, cells at 50% confluency were transfected using Lipofectamine 2000 (Invitrogen) according to the manufacturer's instructions. Cells were typically used for experiments 18 h after transfection. Rab31 (MSS272451, MSS272452, MSS272453) and APPL2 (MSS211085, MSS211087, MSS278056) were silenced using a Stealth siRNAs Primer Set from Life Technologies. Nontargeting siRNA was used as a control. Lipofectamine RNAiMAX was used to transfect RAW 264.7 cells with siRNA according to the manufacturer's instructions (Life Technologies).

Phagocytic assay

Human IgG–conjugated 3-µm latex beads were prepared according to the manufacturer's protocol (Sigma-Aldrich), centrifuged onto cells at 4°C, and incubated at 37°C to synchronize phagocytosis. Phagocytosis was stopped by adding 4% paraformaldehyde before external beads were immunolabeled with goat anti–human IgG-Cy3. The assay was carried out as previously described (Yeo *et al.*, 2013).

Immunofluorescence, fluorescence microscopy, and live-cell imaging

Immunofluorescence staining was performed as previously described (Pagan *et al.*, 2003). Cells were permeabilized using 0.1% Triton X-100 for 5 min, then incubated with primary and secondary antibodies. Coverslips were mounted in ProLong Gold reagent (Life Technologies) before imaging. For live-cell and fixed-cell imaging experiments, RAW 264.7 macrophages were cultured on glass-bottom, 35-mm dishes (MatTek) and in 24-well culture dishes (Thermo Scientific) with coverslips, respectively. Epifluorescence still images were taken with a 12-Mp differential contrast Roper CoolSNAP HQ2 monochrome camera (DP71; Olympus) using a Personal Deltavision Olympus IX71 inverted wide-field deconvolution microscope fitted for a 60×/numerical aperture (NA) 1.35 oil objective using the associated DPController software (version 2.1; Olympus). Imaging Z-stacks of fixed cells was set at 0.2 µm while imaging of live cells was set at 0.3 µm Z-stack and a 15 s time-lapse interval for 20 min.

Cryo–electron microscopy

For cryo–electron microscopy, phagocytosis in RAW 264.7 macrophages was carried out for 15 min. Cells were fixed in paraformaldehyde and embedded in warm gelatin. Thin sections were cut using a Reichert FCS cryomicrotome at −120°C and immunolabeled by placing the sections on sequential drops of glycine, bovine serum albumin, primary antibody (GFP), and then protein A–gold (5 nm)–conjugated secondary antibody. Sections were viewed on a JEOL 1011 transmission electron microscope at 80 kV, and images were captured using iTEM image software.

Preparation of GTP-bound forms of the Rab31

Nucleotide exchange of GST-Rab31 was performed as described earlier (Simon *et al.*, 1996).

Preparation of cell lysates, SDS–PAGE, Western blotting, and real-time quantitative PCR

Immunoblotting was performed as described previously (Murray *et al.*, 2005b). Briefly, cells were lysed in lysis buffer (20 mM 4-(2-hydroxyethyl)-1-piperazineethanesulfonic acid, pH 7.4, 100 mM NaCl, 1% Igepal [Nonidet-P40; Sigma-Aldrich], 1 mM phenylmethylsulfonyl fluoride [PMSF], 1 mM dithiothreitol [DTT], and complete protease inhibitors [Roche Applied Science]). For Western blotting analysis of p-Akt (Ser-473), p-p38 MAPK (Thr-180/Tyr-182), GAPDH, GFP, Akt, p38 MAPK APPL2, and Rab31, cell lysates were loaded onto 10% SDS–PAGE gels and then transferred onto polyvinylidene fluoride membranes (Immobilon-FL; Millipore) according to the manufacturer's instructions.

Total RNA was prepared using RNeasy mini-kits (Qiagen, Valencia, CA) and then reverse transcribed to cDNA using 1 µg of total RNA, Superscript III reverse transcriptase (Invitrogen, Carlsbad, CA), and an oligo-dT primer. Gene expression was quantified by real-time PCR using SYBR Green PCR master mix (Applied Biosystems) according to previous studies (Schroder *et al.*, 2012), using an ABI Prism 7000 sequence detection system (Applied Biosystems, Foster City, CA). Real-time primers used for mouse Rab31 were CGGGAGCTCAAAGTGTGTCT (left) and CCAATAGTGGGGCTGATGTT (right) and for hypoxanthine-guanine phosphoribosyltransferase (HPRT) were GGAGCGGTAGCACCTCCT (left)

and CATAACCTGGTTCATCATCGC (right). cDNA levels during the linear phase of amplification were normalized against the HPRT gene.

Pull-down and immunoprecipitation experiments

For mass spectrometry analysis, total RAW 264.7 macrophage extracts were lysed in ice-cold lysis buffer. The lysate was centrifuged at 75,600 × *g* for 15 min at 4°C. The supernatant was precleared by the addition of GSH-Sepharose beads for 1 h and pelleted at 50 × *g* for 5 min at 4°C, and the supernatant was collected. Various GST-tagged recombinant proteins were then incubated with an equal amount of tissue lysate at 4°C for 1 h. Beads were washed extensively with ice-cold 20 mM Tris, pH 7.4, containing 150 mM NaCl, 1 mM DTT, and 1 mM PMSF, eluted in 2× SDS–PAGE sample buffer, resolved on 7.5–15% gradient SDS gels, and stained with colloidal Coomassie blue. Identification of proteins was by liquid chromatography–tandem mass spectrometry in the IMB's Mass Spectrometry Facility, University of Queensland. For GFP-nanotrap, experiments were carried out as described previously (Luo *et al.*, 2014b). Briefly, macrophage lysates containing GFP, GFP-Rab31, and GFP-Rab5a, respectively, were incubated with GFP-nanotrap beads and washed with lysis buffer. Complexes were eluted with 2× sample buffer, and protein samples were analyzed on 10% SDS–PAGE gels.

Image analysis software

Imaging analysis of all other data were performed using ImageJ software (version 1.43; National Institutes of Health, Bethesda, MD) and Photoshop CS6 (Adobe).

Statistical analysis

Statistics were calculated using Prism, version 7.0 (GraphPad Software, San Diego, CA). For all experiments in this study, Student's *t* tests (Shapiro–Wilk test) were used unless stated otherwise. One-way analysis of variance was used for posttest analysis of multiple comparisons by Dunnett's method, *$p < 0.05$; **$p < 0.01$; ***$p < 0.001$; ****$p < 0.0001$.

ACKNOWLEDGMENTS

We thank Juliana Venturato and Tatiana Khromykh for expert technical assistance and our colleagues as acknowledged for reagents. Electron microscopy was carried out by Darren Brown. Imaging was performed in the Australian Cancer Research Foundation–funded Cancer Biology Imaging Facility at the Institute for Molecular Bioscience. This work was supported by a funded program (606788), project (569543), and fellowship funding to J.L.S. from the Australian National Health and Medical Research Council.

REFERENCES

Aksoy E, Taboubi S, Torres D, Delbauve S, Hachani A, Whitehead MA, Pearce WP, Berenjeno IM, Nock G, Filloux A, *et al.* (2012). The p110 delta isoform of the kinase PI(3)K controls the subcellular compartmentalization of TLR4 signaling and protects from endotoxic shock. Nat Immunol 13, 1045–1054.

Araki N, Hatae T, Furukawa A, Swanson JA (2003). Phosphoinositide-3-kinase-independent contractile activities associated with Fc gamma-receptor-mediated phagocytosis and macropinocytosis in macrophages. J Cell Sci 116, 247–257.

Bohdanowicz M, Balkin DM, De Camilli P, Grinstein S (2012). Recruitment of OCRL and Inpp5B to phagosomes by Rab5 and APPL1 depletes phosphoinositides and attenuates Akt signaling. Mol Biol Cell 23, 176–187.

Bohdanowicz M, Grinstein S (2013). Role of phospholipids in endocytosis, phagocytosis, and macropinocytosis. Physiol Rev 93, 69–106.

Burd CG, Emr SD (1998). Phosphatidylinositol(3)-phosphate signaling mediated by specific binding to RING FYVE domains. Mol Cell 2, 157–162.

Chial HJ, Lenart P, Chen YQ (2010). APPL proteins FRET at the BAR: direct observation of APPL1 and APPL2 BAR domain-mediated interactions on cell membranes using FRET microscopy. PLoS One 5, 12471.

Chial HJ, Wu R, Ustach CV, McPhail LC, Mobley WC, Chen YQ (2008). Membrane targeting by APPL1 and APPL2: dynamic scaffolds that oligomerize and bind phosphoinositides. Traffic 9, 215–229.

Chua CEL, Tang BL (2014). Engagement of the small GTPase Rab31 protein and its effector, early endosome antigen 1, is important for trafficking of the ligand-bound epidermal growth factor receptor from the early to the late endosome. J Biol Chem 289, 12375–12389.

Collins BM, Skinner CF, Watson PJ, Seaman MNJ, Owen DJ (2005). Vps29 has a phosphoesterase fold that acts as a protein interaction scaffold for retromer assembly. Nat Struct Mol Biol 12, 594–602.

Cox D, Lee DJ, Dale BM, Calafat J, Greenberg S (2000). A Rab11-containing rapidly recycling compartment in macrophages that promotes phagocytosis. Proc Natl Acad Sci USA 97, 680–685.

Cox D, Tseng CC, Bjekic G, Greenberg S (1999). A requirement for phosphatidylinositol 3-kinase in pseudopod extension. J Biol Chem 274, 1240–1247.

Currie RA, Walker KS, Gray A, Deak M, Casamayor A, Downes CP, Cohen P, Alessi DR, Lucocq J (1999). Role of phosphatidylinositol 3,4,5-trisphosphate in regulating the activity and localization of 3-phosphoinositide-dependent protein kinase-1. Biochem J 337, 575–583.

Dewitt S, Tian W, Hallett MB (2006). Localised PtdIns(3,4,5)P-3 or PtdIns(3,4)P-2 at the phagocytic cup is required for both phagosome closure and Ca2+ signalling in HL60 neutrophils. J Cell Sci 119, 443–451.

Diekmann Y, Seixas E, Gouw M, Tavares-Cadete F, Seabra MC, Pereira-Leal JB (2011). Thousands of rab GTPases for the cell biologist. PLoS Comput Biol 7, e1002217.

Egami Y, Fukuda M, Araki N (2011). Rab35 regulates phagosome formation through recruitment of ACAP2 in macrophages during Fc gamma R-mediated phagocytosis. J Cell Sci 124, 3557–3567.

Erdmann KS, Mao Y, McCrea HJ, Zoncu R, Lee S, Paradise S, Modregger J, Biemesderfer D, Toomre D, De Camilli P (2007). A role of the Lowe syndrome protein OCRL in early steps of the endocytic pathway. Dev Cell 13, 377–390.

Flannagan RS, Harrison RE, Yip CM, Jaqaman K, Grinstein S (2010). Dynamic macrophage "probing" is required for the efficient capture of phagocytic targets. J Cell Biol 191, 1205–1218.

Flannagan RS, Jaumouille V, Grinstein S (2012). The cell biology of phagocytosis. Annu Rev Pathol 7, 61–98.

Fratti RA, Backer JM, Gruenberg J, Corvera S, Deretic V (2001). Role of phosphatidylinositol 3-kinase and Rab5 effectors in phagosomal biogenesis and mycobacterial phagosome maturation arrest. J Cell Biol 154, 631–644.

Gratton J-P, Morales-Ruiz M, Kureishi Y, Fulton D, Walsh K, Sessa WC (2001). Akt down-regulation of p38 signaling provides a novel mechanism of vascular endothelial growth factor-mediated cytoprotection in endothelial cells. J Biol Chem 276, 30359–30365.

Grinstein S (2010). Imaging signal transduction during phagocytosis: phospholipids, surface charge, and electrostatic interactions. Am J Phys Cell Phys 299, C876–C881.

Gutierrez MG (2013). Functional role(s) of phagosomal Rab GTPases. Small GTPases 4, 148–158.

Haglund CM, Welch MD (2011). Pathogens and polymers: microbe-host interactions illuminate the cytoskeleton. J Cell Biol 195, 7–17.

Hume DA, Gordon S (1982). Regulation of bone-marrow macrophage proliferation. Adv Exp Med Biol 155, 261–266.

Jaumouillé V, Farkash Y, Jaqaman K, Das R, Clifford Lowell A, Grinstein S (2014). Actin cytoskeleton reorganization by Syk regulates Fcγ receptor responsiveness by increasing its lateral mobility and clustering. Dev Cell 29, 534–546.

Jutras I, Houde M, Currier N, Boulais J, Duclos S, LaBoissiere S, Bonneil E, Kearney P, Thibault P, Pararnithiotis E, *et al.* (2008). Modulation of the phagosome proteome by interferon-gamma. Mol Cell Proteomics 7, 697–715.

Kinchen JM, Doukoumetzidis K, Almendinger J, Stergiou L, Tosello-Trampont A, Sifri CD, Hengartner MO, Ravichandran KS (2008). A pathway for phagosome maturation during engulfment of apoptotic cells. Nat Cell Biol 10, 556–566.

King GJ, Stockli J, Hu S-H, Winnen B, Duprez WGA, Meoli CC, Junutula JR, Jarrott RJ, James DE, Whitten AE, Martin JL (2012). Membrane curvature protein exhibits interdomain flexibility and binds a small GTPase. J Biol Chem 287, 40996–41006.

Lee JS, Nauseef WM, Moeenrezakhanlou A, Sly LM, Noubir S, Leidal KG, Schlomann JM, Krystal G, Reiner NE (2007). Monocyte p110 alpha phosphatidylinositol 3-kinase regulates phagocytosis, the phagocyte oxidase, and cytokine production. J Leukoc Biol 81, 1548–1561.

Leverrier Y, Okkenhaug K, Sawyer C, Bilancio A, Vanhaesebroeck B, Ridley AJ (2003). Class I phosphoinositide 3-kinase p110 beta is required for apoptotic cell and Fc gamma receptor-mediated phagocytosis by macrophages. J Biol Chem 278, 38437–38442.

Liao Y, Hung MC (2003). Regulation of the activity of p38 mitogen-activated protein kinase by Akt in cancer and adenoviral protein E1A-mediated sensitization to apoptosis. Mol Cell Biol 23, 6836–6848.

Lodhi IJ, Chiang S-H, Chang L, Vollenweider D, Watson RT, Inoue M, Pessin JE, Saltiel AR (2007). Gapex-5, a Rab31 guanine nucleotide exchange factor that regulates Glut4 trafficking in adipocytes. Cell Metab 5, 59–72.

Loovers HM, Kortholt A, Groote H de, Whitty L, Nussbaum RL, Haastert PJM van (2007). Regulation of phagocytosis in Dictyostelium by the inositol 5-phosphatase OCRL homolog Dd5P4. Traffic 8, 618–628.

Lu N, Shen Q, Mahoney TR, Neukomm LJ, Wang Y, Zhou Z (2012). Two PI 3-kinases and one PI 3-phosphatase together establish the cyclic waves of phagosomal PtdIns(3)P critical for the degradation of apoptotic cells. PLoS Biol 10, e1001245.

Luo L, King NP, Yeo JC, Jones A, Stow JL (2014a). Single-step protease cleavage elution for identification of protein–protein interactions from GST pull-down and mass spectrometry. Proteomics 14, 19–23.

Luo L, Wall AA, Yeo JC, Condon ND, Norwood SJ, Schoenwaelder S, Chen KW, Jackson S, Jenkins BJ, Hartland EL, *et al*. (2014b). Rab8a interacts directly with PI3Kγ to modulate TLR4-driven PI3K and mTOR signalling. Nat Commun 5, 4407.

Marion S, Mazzolini J, Herit F, Bourdoncle P, Kambou-Pene N, Hailfinger S, Sachse M, Ruland J, Benmerah A, Echard A, *et al*. (2012). The NF-κB signaling protein Bcl10 regulates actin dynamics by controlling AP1 and OCRL-bearing vesicles. Dev Cell 23, 954–967.

Miaczynska M, Christoforidis S, Giner A, Shevchenko A, Uttenweiler-Joseph S, Habermann B, Wilm M, Parton RG, Zerial M (2004). APPL proteins link Rab5 to nuclear signal transduction via an endosomal compartment. Cell 116, 445–456.

Mitsuuchi Y, Johnson SW, Sonoda G, Tanno S, Golemis EA, Testa JR (1999). Identification of a chromosome 3p14.3-21.1 gene, APPL, encoding an adaptor molecule that interacts with the oncoprotein-serine/threonine kinase AKT2. Oncogene 18, 4891–4898.

Murray RZ, Kay JG, Sangermani DG, Stow JL (2005a). A role for the phagosome in cytokine secretion. Science 310, 1492–1495.

Murray RZ, Wylie FG, Khromykh T, Hume DA, Stow JL (2005b). Syntaxin 6 and Vti1b form a novel SNARE complex, which is up-regulated in activated macrophages to facilitate exocytosis of tumor necrosis Factor-alpha. J Biol Chem 280, 10478–10483.

Nechamen CA, Thomas RM, Dias JA (2007). APPL1, APPL2, Akt2 and FOXO1a interact with FSHR in a potential signaling complex. Mol Cell Endocrinol 260, 93–99.

Ng EL, Ng JJ, Liang F, Tang BL (2009). Rab22B is expressed in the CNS astroglia lineage and plays a role in epidermal growth factor receptor trafficking in A431 cells. J Cell Physiol 221, 716–728.

Pagan JK, Wylie FG, Joseph S, Widberg C, Bryant NJ, James DE, Stow JL (2003). The t-SNARE syntaxin 4 is regulated during macrophage activation to function in membrane traffic and cytokine secretion. Curr Biol 13, 156–160.

Patel PC, Harrison RE (2008). Membrane ruffles capture C3bi-opsonized particles in activated macrophages. Mol Biol Cell 19, 4628–4639.

Pyrzynska B, Banach-Orlowska M, Teperek-Tkacz M, Miekus K, Drabik G, Majka M, Miaczynska M (2013). Multifunctional protein APPL2 contributes to survival of human glioma cells. Mol Oncol 7, 67–84.

Rane MJ, Song Y, Jin S, Barati MT, Wu R, Kausar H, Tan Y, Wang Y, Zhou G, Klein JB, *et al*. (2010). Interplay between Akt and p38 MAPK pathways in the regulation of renal tubular cell apoptosis associated with diabetic nephropathy. Am J Physiol Renal Physiol 298, F49–F61.

Rashid S, Pilecka I, Torun A, Olchowik M, Bielinska B, Miaczynska M (2009). Endosomal adaptor proteins APPL1 and APPL2 are novel activators of beta-catenin/TCF-mediated transcription. J Biol Chem 284, 18115–18128.

Rodriguez-Gabin AG, Cammer M, Almazan G, Charron M, Larocca JN (2001). Role of rRAB22b, an oligodendrocyte protein, in regulation of transport of vesicles from trans Golgi to endocytic compartments. J Neurosci Res 66, 1149–1160.

Rodriguez-Gabin AG, Ortiz E, Demoliner K, Si Q, Almazan G, Larocca JN (2010). Interaction of Rab31 and OCRL-1 in oligodendrocytes: its role in transport of mannose 6-phosphate receptors. J Neurosci Res 88, 589–604.

Schenck A, Goto-Silva L, Collinet C, Rhinn M, Giner A, Habermann B, Brand M, Zerial M (2008). The endosomal protein Appl1 mediates akt substrate specificity and cell survival in vertebrate development. Cell 133, 486–497.

Schroder K, Irvine KM, Taylor MS, Bokil NJ, Cao KAL, Masterman KA, Labzin LI, Semple CA, Kapetanovic R, Fairbairn L, *et al*. (2012). Conservation and divergence in Toll-like receptor 4-regulated gene expression in primary human versus mouse macrophages. Proc Natl Acad Sci USA 109, E944–E953.

Scott CC, Dobson W, Botelho RJ, Coady-Osberg N, Chavrier P, Knecht DA, Heath C, Stahl P, Grinstein S (2005). Phosphatidylinositol-4,5-bisphosphate hydrolysis directs actin remodeling during phagocytosis. J Cell Biol 169, 139–149.

Seto S, Tsujimura K, Koide Y (2011). Rab GTPases regulating phagosome maturation are differentially recruited to mycobacterial phagosomes. Traffic 12, 407–420.

Shim J, Lee S-M, Lee MS, Yoon J, Kweon H-S, Kim Y-J (2010). Rab35 mediates transport of Cdc42 and Rac1 to the plasma membrane during phagocytosis. Mol Cell Biol 30, 1421–1433.

Shurety W, Merino-Trigo A, Brown D, Hume DA, Stow JL (2000). Localization and post-Golgi trafficking of tumor necrosis factor-alpha in macrophages. J Interferon Cytokine Res 20, 427–438.

Silver KE, Harrison RE (2011). Kinesin 5B is necessary for delivery of membrane and receptors during Fc gamma R-mediated phagocytosis. J Immunol 186, 816–825.

Simon I, Zerial M, Goody RS (1996). Kinetics of interaction of Rab5 and Rab7 with nucleotides and magnesium ions. J Biol Chem 271, 20470–20478.

Smith AC, Heo W Do, Braun V, Jiang X, Macrae C, Casanova JE, Scidmore MA, Grinstein S, Meyer T, Brumell JH (2007). A network of Rab GTPases controls phagosome maturation and is modulated by Salmonella enterica serovar Typhimurium. J Cell Biol 176, 263–268.

Stein M-P, Mueller MP, Wandinger-Ness A (2012). Bacterial pathogens commandeer Rab GTPases to establish intracellular niches. Traffic 13, 1565–1588.

Swanson JA, Hoppe AD (2004). The coordination of signaling during Fc receptor-mediated phagocytosis. J Leukoc Biol 76, 1093–1103.

Tamura N, Hazeki K, Okazaki N, Kametani Y, Murakami H, Takaba Y, Ishikawa Y, Nigorikawa K, Hazeki O (2009). Specific role of phosphoinositide 3-kinase p110 alpha in the regulation of phagocytosis and pinocytosis in macrophages. Biochem J 423, 99–108.

Tan Y, You H, Coffey FJ, Wiest DL, Testa JR (2010a). Appl1 is dispensable for Akt signaling in vivo and mouse T-cell development. Genesis 48, 531–539.

Tan Y, You H, Wu C, Altomare DA, Testa JR (2010b). Appl1 is dispensable for mouse development, and loss of Appl1 has growth factor-selective effects on Akt signaling in murine embryonic fibroblasts. J Biol Chem 285, 6377–6389.

Tushinski RJ, Oliver IT, Guilbert LJ, Tynan PW, Warner JR, Stanley ER (1982). Survival of mononuclear phagocytes depends on a lineage-specific growth-factor that the differentiated cells selectively destroy. Cell 28, 71–81.

Urbanska A, Sadowski L, Kalaidzidis Y, Miaczynska M (2011). Biochemical characterization of APPL endosomes: the role of annexin A2 in APPL membrane recruitment. Traffic 12, 1227–1241.

Vieira OV, Botelho RJ, Rameh L, Brachmann SM, Matsuo T, Davidson HW, Schreiber A, Backer JM, Cantley LC, Grinstein S (2001). Distinct roles of class I and class III phosphatidylinositol 3-kinases in phagosome formation and maturation. J Cell Biol 155, 19–25.

Vieira OV, Bucci C, Harrison RE, Trimble WS, Lanzetti L, Gruenberg J, Schreiber AD, Stahl PD, Grinstein S (2003). Modulation of Rab5 and Rab7 recruitment to phagosomes by phosphatidylinositol 3-kinase. Mol Cell Biol 23, 2501–2514.

Wang CH, Xin XB, Xiang RH, Ramos FJ, Liu ML, Lee HJ, Chen HZ, Mao XM, Kikani CK, Liu F, Dong LQ (2009). Yin-yang regulation of adiponectin signaling by APPL isoforms in muscle cells. J Biol Chem 284, 31608–31615.

Wang Y-B, Wang J-J, Wang S-H, Liu S-S, Cao J-Y, Li X-M, Qiu S, Luo J-H (2012). Adaptor protein APPL1 couples synaptic NMDA receptor with neuronal prosurvival phosphatidylinositol 3-kinase/Akt pathway. J Neurosci 32, 11919–11929.

Watton SJ, Downward J (1999). Akt/PKB localisation and 3′ phosphoinositide generation at sites of epithelial cell–matrix and cell–cell interaction. Curr Biol 9, 433–436.

Yeo JC, Wall AA, Stow JL, Hamilton NA (2013). High-throughput quantification of early stages of phagocytosis. Biotechniques 55, 115–124.

Zhu G, Chen J, Liu J, Brunzelle JS, Huang B, Wakeham N, Terzyan S, Li X, Rao Z, Li G, Zhang XC (2007). Structure of the APPL1 BAR-PH domain and characterization of its interaction with Rab5. EMBO J 26, 3484–3493.

Zoncu R, Perera RM, Balkin DM, Pirruccello M, Toomre D, De Camilli P (2009). A phosphoinositide switch controls the maturation and signaling properties of APPL endosomes. Cell 136, 1110–1121.